

# Effect of higher orbital angular momenta in the baryon spectrum

H. Garcilazo<sup>(1)</sup>, A. Valcarce<sup>(2,3)</sup> and F. Fernández<sup>(2)</sup>

(1) *Escuela Superior de Física y Matemáticas*

*Instituto Politécnico Nacional, Edificio 9, 07738 México D.F., Mexico*

(2) *Grupo de Física Nuclear*

*Universidad de Salamanca, E-37008 Salamanca, Spain*

(3) *Departamento de Física Teórica,*

*Universidad de Valencia, E-46100 Valencia, Spain*

## Abstract

We have performed a Faddeev calculation of the baryon spectrum for the chiral constituent quark model including higher orbital angular momentum states. We have found that the effect of these states is important, although a description of the baryon spectrum of the same quality as the one given by including only the lowest-order configurations can be obtained. We have studied the effect of the pseudoscalar quark-quark interaction on the relative position of the positive- and negative-parity excitations of the nucleon as well as the effect of varying the strength of the color-magnetic interaction.

Keywords:

non-relativistic quark models, baryon spectrum, Faddeev calculations

Pacs:

12.39.Jh, 14.20.-c

In a recent paper [1] we calculated the nonstrange baryon spectrum within a Faddeev approach for the chiral constituent quark model [2,3,4,5]. This model, besides a confining interaction and a perturbative one-gluon exchange, includes a pseudoscalar and a scalar boson exchange between quarks. In Ref. [1] only the lowest-order configurations  $(\ell, \lambda, s, t)$  ( $\ell$  is the orbital angular momentum of a pair,  $\lambda$  is the orbital angular momentum between the pair and the third particle, while  $s$  and  $t$  are the spin and isospin of the pair) were included. Thus, for the  $N1/2^+$  state (corresponding to the  $N$  and to the  $N(1440)$ ) we included the two configurations  $(0,0,0,0)$  and  $(0,0,1,1)$ . For the  $N1/2^-$  state (the  $N(1535)$ ) we included the four configurations  $(0,1,0,0)$ ,  $(0,1,1,1)$ ,  $(1,0,1,0)$ , and  $(1,0,0,1)$ , while for the  $\Delta3/2^+$  state (the  $\Delta$ ) we included the single configuration  $(0,0,1,1)$ . We have now extended our calculation to include all the configurations  $(\ell, \lambda, s, t)$  with  $\ell$  and  $\lambda$  up to 5. The objective of the present work is to evaluate the effects of the higher orbital angular momentum components in a model including gluon as well as Goldstone boson exchanges

To study the convergence behavior with respect to the number of  $(\ell, \lambda, s, t)$  configurations we give in Table I the results for the  $\Delta$ ,  $N(1535)$ ,  $N$ , and  $N(1440)$ , corresponding to Fig. 4 of Ref. [1]. In this table we give the mass difference with respect to the nucleon ground state including 12  $(\ell, \lambda, s, t)$  configurations, i.e. with  $\ell$  and  $\lambda$  up to 5, considered to be the converged result for the nucleon ground state and therefore our mass reference. As can be seen, the convergence with respect to the number of configurations is different for different states, so that, for example, the  $\Delta$  comes down by only 5 MeV while the  $N(1535)$ ,  $N$ , and  $N(1440)$  they all come down by approximately 100 MeV when one includes the higher orbital angular momentum configurations. It is also interesting to notice that while in the lowest-order calculation the  $N(1440)$  lies below the  $N(1535)$ , when one includes the higher orbital angular momenta the situation is reversed. We will return to this point later on. The same study could be done in the case of Figs. 1-3 of Ref. [1]. However, the results would be similar to those reported on Table I, although the effect of the higher orbital angular momentum components is smaller in these cases. The reason for this stems from the fact that the one-pion exchange (OPE) force is weaker in these cases, and therefore the contribution of higher orbital angular momenta is less important.

As a consequence of the previous results, it is clear that the calculation of Ref. [1] was done in a restricted Hilbert space neglecting orbital angular momentum components that are important to obtain a conclusion about the performance of the model under discussion. It therefore arises the question if the model of Ref. [1] can produce a reasonable baryon spectrum when all the relevant Hilbert space components are included. We want to show that similar fits for the baryon spectrum can be obtained with the extended Faddeev calculation as those obtained with the lowest-order version used to calculate the results of Ref. [1]. As an example, we show in Fig. 1 the baryon spectrum obtained using the parameters of Table II when the higher orbital angular momentum configurations are included. In this figure we plot by the solid line the excitation energy with respect to the nucleon ground state. The shaded areas correspond to the experimental value including its uncertainty. As one can see from this figure, the relative position of the positive-parity states  $N$ ,  $\Delta$ , and  $N(1440)$  are correctly given, although the negative-parity states lie below the experimental results as is well-known to happen for models of this kind. The parameters of Table II, which gave rise to this spectrum, are the ones that have been used in the chiral constituent quark model for the description of the baryon-baryon interaction [2,3]. The parameter  $r_0$  has been taken

as 0.25 fm, a typical value for spectroscopic models, such that the delta function of the OGE interaction is regularized in the region of short distances. The slope of the confining potential,  $a_c$ , which in Table II is 67.0 MeV fm<sup>-1</sup>, is not so different from the value 72.5 MeV fm<sup>-1</sup> used in most of the previous applications of the model to the baryon spectrum [4,5]. (One should not forget at this point that consistency with the two-nucleon sector does not impose any restriction to the value of  $a_c$ , because the confining interaction does not contribute to the nucleon-nucleon potential.) This does not mean, however, that the fit of the spectrum requires the parameters to be close to those of Table II. It is possible to find equally good fits with quite different sets of parameters. We show in Fig. 2 the spectrum obtained with the parameters of Table III, which differ considerably from those of Table II.

As can be seen in Figs. 1 and 2, with two different sets of parameters for confinement and the one-gluon exchange, fits of a similar quality are obtained. In both cases one observes how the relative position of the positive and negative parity excitations of the nucleon are reversed with respect to the experimental order. This has been stated as a basic deficiency of models with a strong one-gluon exchange interaction. In order to check if the responsible for this incorrect ordering is the one-gluon exchange, we have calculated the energy of the  $N(1440)$  and the  $N(1535)$  starting with the set of parameters of Table II and varying the contribution of the color-magnetic interaction by modifying the coupling constant  $\alpha_s$  of the OGE interaction. The results are shown in Fig. 3. As we are interested in the relative energy of the positive and negative parity excitations of the nucleon, we have plotted directly the absolute value obtained from our code. In this case the relative position of the  $N(1440)$  and the  $N(1535)$  is not very much affected by the modification of  $\alpha_s$ . This behavior indicates that the correct level ordering between the negative and positive parity excited states of the nucleon is not connected with the lack of OGE. Moreover, a suppression of the OGE, would imply a stronger pseudoscalar interaction in order to reproduce the  $N - \Delta$  mass difference, and therefore one would obtain a model that it is incompatible with the understanding of the basic features of the two-nucleon system [6].

As has been explained in Ref. [1], a possible mechanism responsible for the inversion of these states can be obtained through the pseudoscalar interaction. To illustrate this point we have again calculated the energy of the  $N(1440)$  and the  $N(1535)$  starting with the set of parameters of Table II, but increasing in this case the contribution of the pseudoscalar interaction by letting the cutoff parameter  $\Lambda_\pi$  of the OPE to increase. The results are shown in Fig. 4, where we have again plotted directly the absolute value obtained from our code. As can be seen, the inversion of the ordering between the positive and negative parity states can be achieved if  $\Lambda_\pi$  becomes sufficiently large (around 7 fm<sup>-1</sup> for the set of parameters of Table II). One should also mention that a model with such a strong cutoff for the OPE is not realistic. In this case the  $N - \Delta$  mass difference is around 955 MeV. We have fitted again the  $N - \Delta$  mass difference by modifying the confinement constant and suppressing the OGE. In this case we lose again the inversion between the negative and positive parity states. Let at this point make a comment about the smaller influence of the higher orbital angular momentum components in the case of Figs. 1-3 of Ref. [1] that we have mentioned previously. The larger the cut-off of the pseudoscalar interaction, the larger the nucleon-delta mass difference. This effect is obtained because the energy of the nucleon ground state is decreased, enhancing in this way the influence of the higher orbital angular momentum components.

As a summary, we want to point out that higher orbital angular momentum components play an important role on the description of the low-energy baryon spectrum. They mainly influence the relative energy of the nucleonic and  $\Delta$  sectors (as illustrated in Table I), but they also affect the relative position of the positive and negative parity excitations of the nucleon. After reanalyzing the results reported on Ref. [1], where these components were not considered, we did not find any qualitative modification of the conclusions obtained there. Therefore, the validity of a model where the OGE is combined with Goldstone-boson exchanges is without any doubt, and it presents advantages with respect to models based only on Goldstone-boson exchanges, as has been recently emphasized in several works [6,7]. In particular, the chiral constituent quark model of Refs. [2,3,4,5] is able to generate a quite reasonable description of the baryon spectrum, with a set of parameters that allows to understand the  $NN$  phenomenology. For the case of the baryon spectrum, the set of parameters we found is not unique, as also stated in Ref. [1], and we did not find any restriction to the value of  $\alpha_s$ . The correct level ordering is closely related to the pseudoscalar interaction and, in the present model, can only be achieved at the expense of losing the correct description of the  $NN$  system. As a consequence, other mechanisms should be responsible for the correct level ordering if consistency with the two-nucleon system is required.

## ACKNOWLEDGMENTS

We like to thank Dr. W. Plessas for enlightening discussions on the subject of this paper. This work has been partially funded by COFAA-IPN (Mexico), by Dirección General de Investigación Científica y Técnica (Spain) under the Contract No. PB97-1410, by Junta de Castilla y León under the Contract No. SA109/01. A. V. thanks the Ministerio de Educación, Cultura y Deporte for financial support through the Salvador de Madariaga program.

## REFERENCES

- [1] H. Garcilazo, A. Valcarce, and F. Fernández, Phys. Rev. C **63**, 035207 (2001).
- [2] F. Fernández, A. Valcarce, U. Straub, and A. Faessler, J. Phys. G **19**, 2013 (1993).
- [3] A. Valcarce, A. Buchmann, F. Fernández, and A. Faessler, Phys. Rev. C **50**, 2246 (1994).
- [4] A. Valcarce, P. González, F. Fernández, and V. Vento, Phys. Lett. B **367**, 35 (1996).
- [5] F. Fernández, P. González, and A. Valcarce, Few-Body Syst. Supp. **10**, 395 (1999).
- [6] C. Nakamoto and H. Toki, Prog. Theor. Phys. **99**, 1001 (1998).
- [7] N. Isgur, Phys. Rev. D **62**, 054026 (2000); nucl-th/0007008.

## FIGURES

FIG. 1. Relative energy nucleon and delta spectrum up to 1.0 GeV excitation energy for the set of parameters of Table II. The solid corresponds to the results of the model of Ref. [1] including  $\ell$  and  $\lambda$  up to 5. The shaded region, whose size stands for the experimental uncertainty, represents the experimental data.

FIG. 2. Same as Fig. 1 for the set of parameters of Table III.

FIG. 3.  $N(1440)$  and  $N(1535)$  mass as a function of the strong coupling constant,  $\alpha_s$ . See text for details.

FIG. 4.  $N(1440)$  and  $N(1535)$  mass as a function of the cutoff mass for the one-pion exchange,  $\Lambda_\pi$ . See text for details.

# TABLES

TABLE I. Convergence of baryon masses with respect to the number (Nr.) of configurations  $(\ell, \lambda, s, t)$ . See text for details.

Nr.	$M_{\Delta}(\text{MeV})$	Nr.	$M_{N(1535)}(\text{MeV})$	Nr.	$M_N(\text{MeV})$	Nr.	$M_{N(1440)}(\text{MeV})$
1	423	4	643	2	115	2	641
2	419	8	601	4	68	4	622
3	418	12	570	6	21	6	587
		16	551	8	12	8	578
		20	540	10	2	10	562
				12	0	12	558

TABLE II. Quark model parameters for the calculation of Fig. 1.

$m_q(\text{MeV})$	313
$\alpha_s$	0.485
$a_c(\text{MeV} \cdot \text{fm}^{-1})$	67.0
$\alpha_{ch}$	0.0269
$r_0(\text{fm})$	0.25
$m_{\sigma}(\text{fm}^{-1})$	3.42
$m_{\pi}(\text{fm}^{-1})$	0.7
$\Lambda_{\pi}(\text{fm}^{-1})$	4.2
$\Lambda_{\sigma}(\text{fm}^{-1})$	4.2

TABLE III. Quark model parameters for the calculation of Fig. 2.

$m_q(\text{MeV})$	313
$\alpha_s$	0.75
$a_c(\text{MeV} \cdot \text{fm}^{-1})$	60.12
$\alpha_{ch}$	0.0269
$r_0(\text{fm})$	0.8
$m_{\sigma}(\text{fm}^{-1})$	3.42
$m_{\pi}(\text{fm}^{-1})$	0.7
$\Lambda_{\pi}(\text{fm}^{-1})$	4.2
$\Lambda_{\sigma}(\text{fm}^{-1})$	4.2

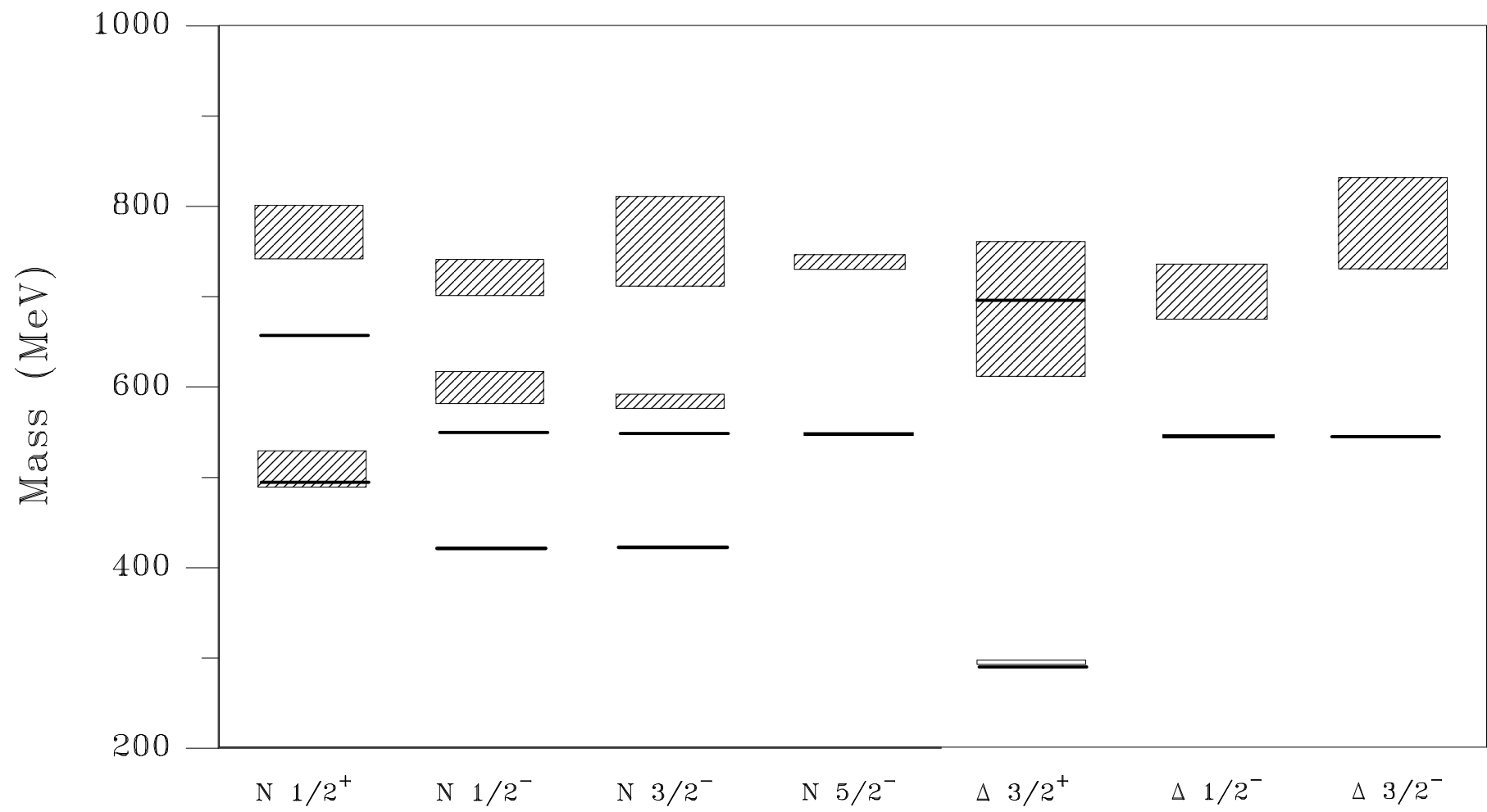


Figure 1



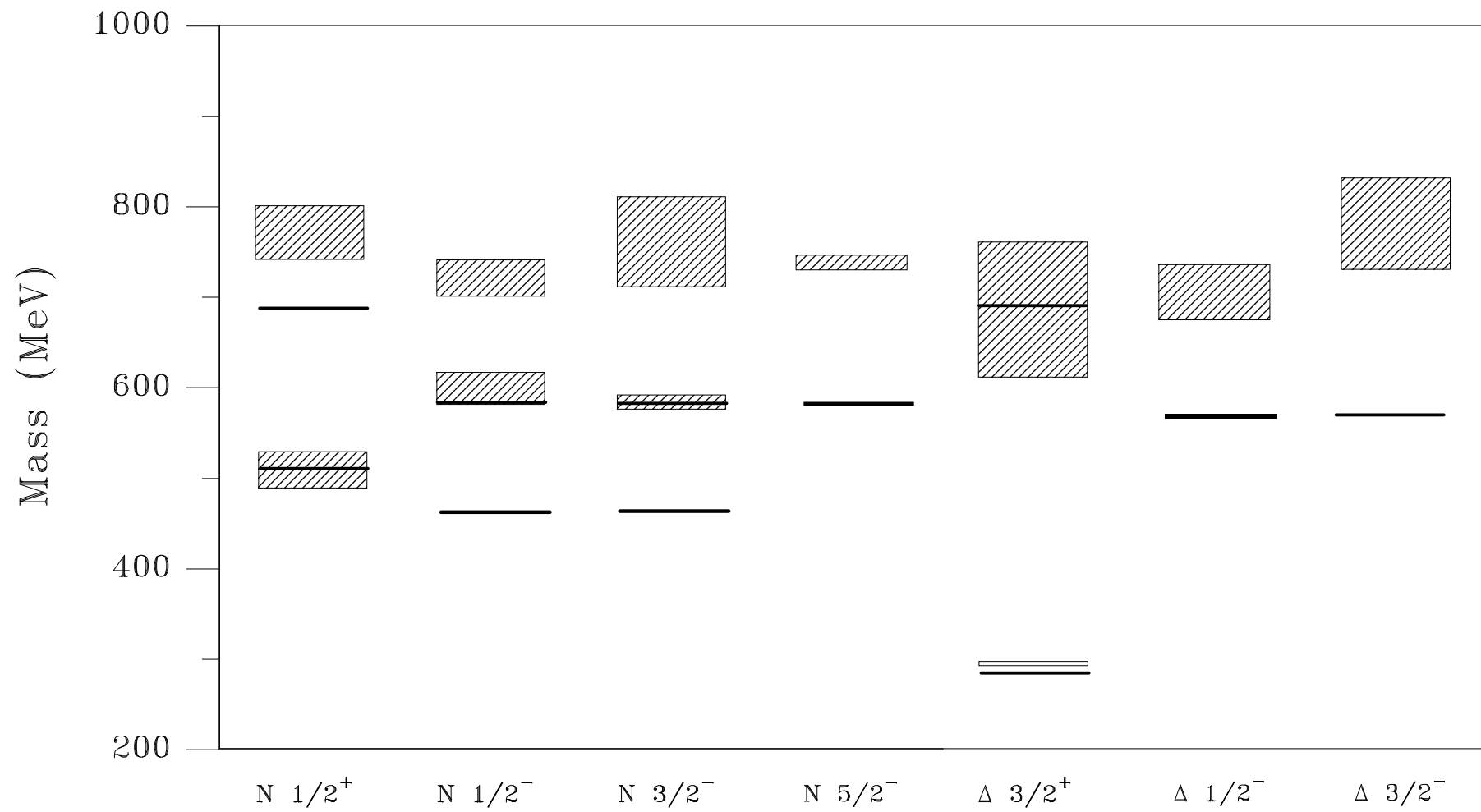


Figure 2

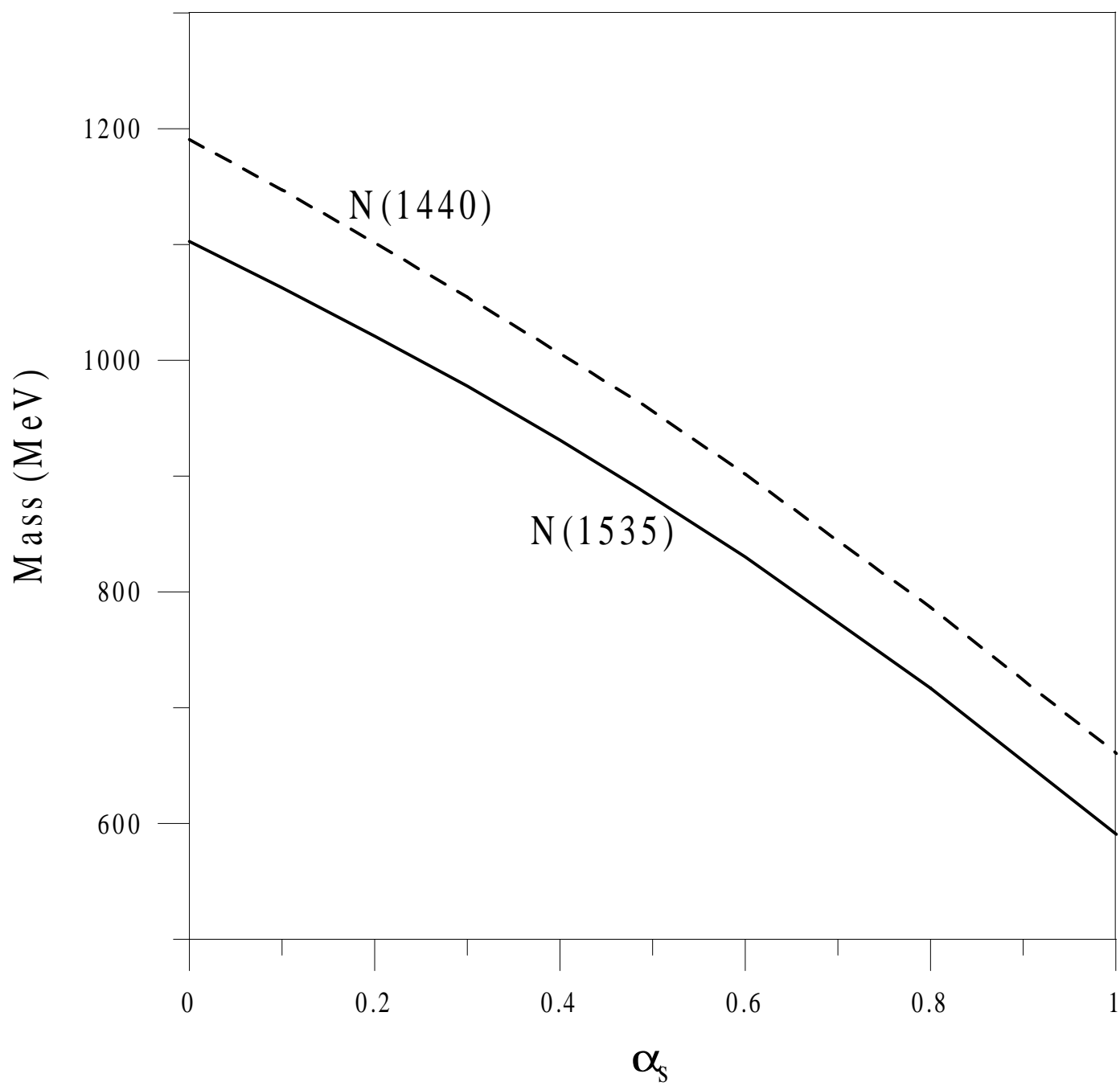


Figure 3

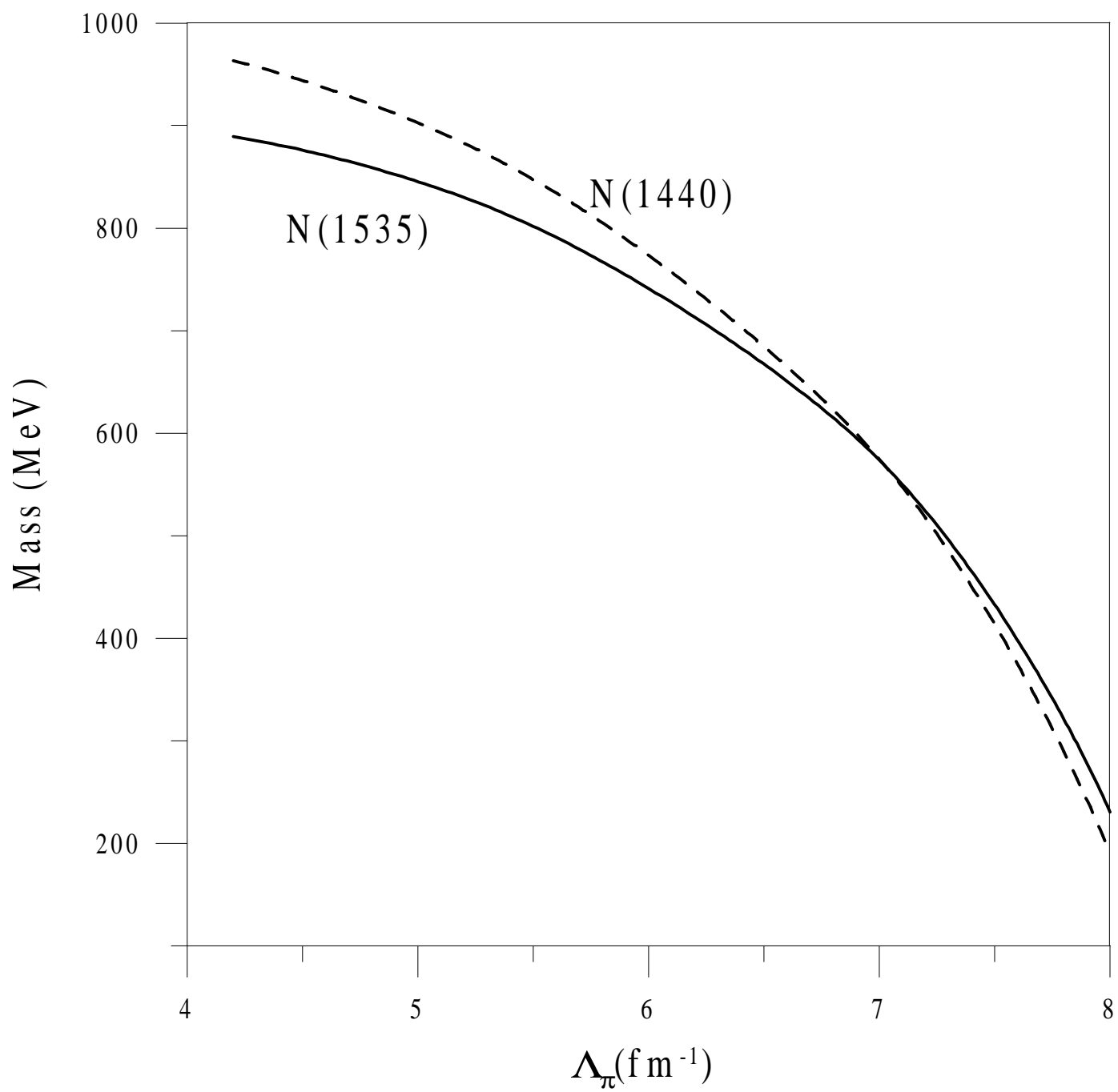


Figure 4